

New series of 4-(4'-octyloxybiphenyl-4-yloxymethyl)benzoic acid derivatives with mesogenic properties

Jadwiga Szydłowska,^{*a} Damian Pocięcha,^a Ewa Górecka,^a Dorota Kardaś,^b Józef Mieczkowski^b and Jan Przedmojski^c

^aLaboratory of Dielectrics and Magnetics, Department of Chemistry, Warsaw University, Al. Żwirki i Wigury 101, 02-089 Warsaw, Poland. E-mail: jadszyd@chem.uw.edu.pl

^bLaboratory of Natural Products Analysis, Department of Chemistry, Warsaw University, ul. Pasteura 1, 00-093 Warsaw, Poland

^cDepartment of Physics, Warsaw Technical University, ul. Koszykowa 75, 00-662 Warsaw, Poland

Received 3rd July 1998, Accepted 21st October 1998

Three homologous series of (4'-octyloxybiphenyl-4-yloxymethyl)benzoic acid derivatives were synthesised and studied. The compounds, substituted by *n*-alkyl esters, reveal strong discrimination of the tilted phases formation upon elongation of the alkyl group. In compounds with 2 methylalkyl chains, tilted phases were exclusively observed with both ferroelectric and antiferroelectric properties. It has been observed that for chiral derivatives an elongation of the chiral chain leads to odd-even effect on the polar properties. Also elongation of non-chiral alkoxy terminal chains affects the polar properties. For short homologues the antiferroelectric phases dominate, while for long homologues only ferroelectric behaviour is observed. The influence of strongly polar lateral groups (Cl, Br, NO₂) attached to the biphenyl ring on LC phase properties was also determined. It was detected that mono-substituted compounds have lower mesogenic stability than their disubstituted counterparts. The effect is probably related to restricted rotation around the phenyl-O bond that leads to a more rigid core structure.

1. Introduction

Synthesis and systematic studies of the liquid crystal properties of several homologous series with (biphenyl-4-yloxymethyl)-phenyl mesogenic cores, in which a biphenyl ring is joined to a phenyl ring by a OCH₂ linkage, were undertaken. In the core structure there are moieties that exhibit competing, favourable or discouraging influences on tilted phase formation. The electron donor alkoxy group and the dipolar acceptor carboxy function (COO) strongly induce tilted phases, while the polar central OCH₂ linkage promotes orthogonal phases. Surprisingly, so far this core structure has been relatively rarely used to obtain mesogenic compounds.¹⁻³ The most comprehensive studies were performed for nitriles and nitro derivatives.¹

In the presented work the core is substituted by alkoxy and ester groups (compounds 5-17 on Scheme 1). The terminal ester moiety has been modified either to enhance or reduce tilted phase formation. Three series 1-3 were studied in detail. The influence of strongly polar lateral groups (Cl, Br, NO₂) on the biphenyl ring on the LC phase properties was also determined.

2. Experimental

The liquid crystalline phases were identified on the basis of routine examinations, namely by observation of created microscopic textures.⁴ For the texture observations a Zeiss Jenapol-U polarising microscope equipped with a Mettler FP82HT hot stage was used. The mesophase identification was supported by X-ray studies that gave crystallographic parameters. The measurements were taken for powder samples with a DRON diffractometer equipped with a graphite monochromator.

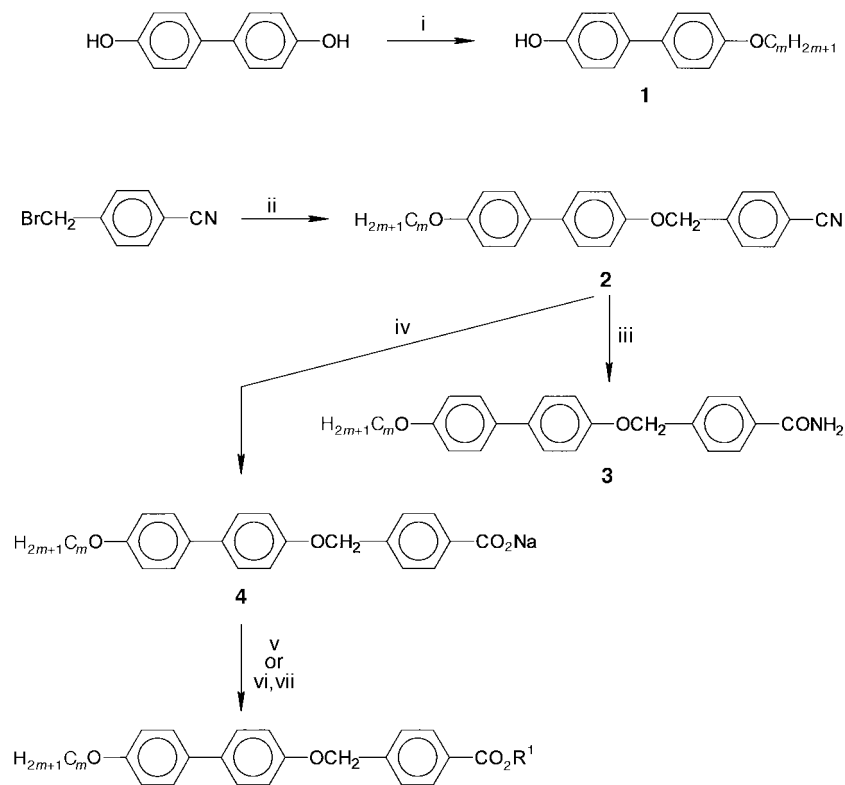
For calorimetric investigations a DSC7 Perkin-Elmer set-up was used. Runs were performed mainly at a scanning rate of 5 K min⁻¹. When necessary, to visualise some thermal effects or in the case of thermally unstable compounds, the scanning

rates were modified and resultant temperatures were recalculated for the standard rate.

The selective reflection wavelength was measured in a polarising microscope Nikon Optiphot2-Pol equipped with a micro-spectrophotometry system working in the transmission mode. The helical twist sense was determined in studies of circularly polarised light transmission through a free suspended film.⁵

The relative permittivity was measured at 120 Hz in 25 μm thick cells, under a temperature sweep of 2 K min⁻¹, using a Wayne Kerr Precision Component Analyzer 6425. For spontaneous polarisation studies the switching current method was applied. The molecular tilt was measured as an angle difference between minimum transmission positions in a planar sample, which was placed under a microscope between crossed polarizers and subjected to opposite dc electric fields. From the direction of the induced tilt angle and the direction of the applied field the spontaneous polarisation (*P_s*) sign was determined. The vector *P_s* is defined as positive⁶ if directed along a vector [*c* × *z*] for (*n* · *z*) > 0, where *n* is the director, *c* is its projection to the smectic layer and *z* is the layer normal. The identification of the polar properties of the phases was based mainly on observations of the apparent tilt and *P_s* electric switching.⁷ The double current peak at spontaneous polarisation reversal and tristable electrooptic switching was detected via low frequency (~1 Hz) measurements of antiferroelectric phases. Additionally the ferroelectric-antiferroelectric phase transition was monitored as a sudden change in the relative permittivity. Molecular dimensions were estimated by molecular modelling (HYPERCHEM 3.0).

In order to confirm the molecular structure of synthesised compounds some analytical methods were applied. Infrared (IR) spectra were obtained using a Nicolet Magna IR 500 spectrophotometer. NMR spectra were recorded on Varian Unity Plus Spectrometer operating at 500 MHz for ¹H NMR and at 125 MHz for ¹³C NMR. Tetramethylsilane was used as an internal standard. Chemical shifts are reported in ppm. TLC analyses were performed on a Merck 60 silica gel glass



- 5** $m = 8$, $\text{R}^1 = \text{C}_n\text{H}_{2n+1}$
6 $m = 7-14, 16$, $\text{R}^1 = \text{CHMeC}_6\text{H}_{13}$
7 $m = 8$, $\text{R}^1 = \text{CHMeC}_n\text{H}_{2n+1}$
8 $m = 8$, $\text{R}^1 = \text{CH}(\text{C}_8\text{H}_{17})_2$
9 $m = 8$, $\text{R}^1 = \text{Bu}^i$
10 $m = 8$, $\text{R}^1 = (\text{CH}_2)_2\text{CHMe}_2$
11 $m = 8$, $\text{R}^1 = \text{CH}_2\text{CHEtBu}$
12 $m = 8$, $\text{R}^1 = \text{CH}_2\text{CH}=\text{CH}_2$
13 $m = 8$, $\text{R}^1 = [(E)\text{-CH}_2\text{CMe}=\text{CHCH}_2]_3\text{H}$
14 $m = 8$, $\text{R}^1 = [(E)\text{-CH}_2\text{CH}=\text{CMeCH}_2]_2\text{H}$
15 $m = 8$, $\text{R}^1 = \text{CH}_2\text{C}\equiv\text{CH}$
16 $m = 8$, $\text{R}^1 = \text{cyclohexyl}$
17 $m = 8$, $\text{R}^1 = \text{CH}_2\text{CCl}_3$

Scheme 1 Reagents and conditions: i, $\text{C}_m\text{H}_{2m+1}\text{Br}$, K_2CO_3 , DMF; ii, **1**, K_2CO_3 , DMF; iii, NaOH, MeOH, reflux; iv, NaOH, BuOH, reflux; v, R^1OH , H_2SO_4 , toluene, reflux; vi, $(\text{COCl})_2$, toluene, reflux; vii, R^1OH , pyridine.

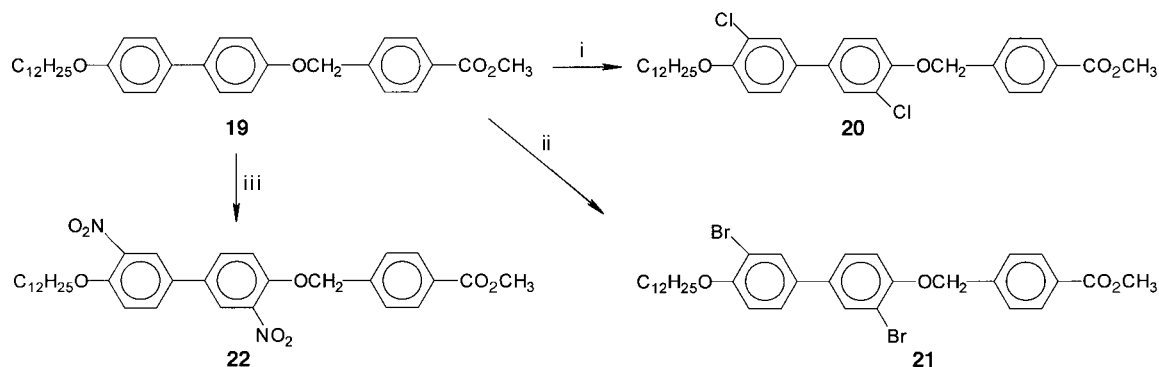
plate and visualised using iodine vapour. The column chromatography was carried out at atmospheric pressure using silica gel (100–200 mesh, Merck).

2.1 Synthesis

Synthetic routes to the described compounds are outlined on Scheme 1 and 2.

4-(4'-Octyloxybiphenyl-4-ylomethyl)benzotrile **2** ($m = 8$).

To 4,4'-dihydroxybiphenyl (50 g, 270 mmol) in dimethylformamide (400 ml), octyl bromide (58 g, 300 mmol) and anhydrous potassium carbonate (42 g, 300 mmol) were added. The mixture was stirred and heated at 100 °C during 4 h, cooled to room temperature, and poured into water. The crude product was crystallised from methanol. The monoalkylated (compound **1** ($m = 8$)) (33 g, 41% yield) and dialkylated (25 g, 23%



Scheme 2 Reagents and conditions: i, Cl_2 , CCl_4 ; ii, Br_2 ; iii, HNO_3 .

yield) products were obtained. Compound **1** ($m=8$) was purified by single crystallisation from methanol and had sufficient purity for the next step.

To 4-hydroxy-4'-octyloxybiphenyl **1** ($m=8$) (30 g, 100 mmol) in dimethylformamide (200 ml), anhydrous potassium carbonate (21 g, 500 mmol) and 4-(bromomethyl)benzonitrile (25 g, 130 mmol) were added, stirred for 2 h at room temperature, then heated at 100 °C during 8 h, cooled, poured into water and extracted six times with toluene. The toluene extracts were dried with anhydrous magnesium sulfate, and the product was chromatographed on silica gel at 40 °C to avoid crystallisation and eluted with toluene (23.7 g; 57%).

Elemental analysis for $C_{28}H_{31}NO_2$: Calc. C 81.35, H 7.50, N 3.38; Found C 81.45, H 7.65, N 3.25%; $\nu_{\max}(\text{KBr})/\text{cm}^{-1}$ 2940, 2830, 2210, 1600, 1500; $\delta_{\text{H}}(\text{CDCl}_3)$ 7.72–7.42 (m, 8H), 7.01–6.88 (t, 4H), 5.14 (s, 2H), 3.97 (t, 2H), 1.88–1.71 (dt, 2H), 1.56–1.22 (m, 12H), 0.889 (t, 3H); $\delta_{\text{C}}(\text{CDCl}_3)$ 158.39, 157.18, 142.54, 134.33, 132.86, 132.38, 127.80, 127.66, 127.52, 118.659, 115.00, 114.75, 111.65, 68.95, 68.0, 31.82, 29.37, 29.29, 29.24, 26.05, 22.05, 14.11.

4-(4'-Octyloxybiphenyl-4-yloxymethyl)benzamide **3** ($m=8$).

To sodium hydroxide (1 g) dissolved in methanol (100 ccm), nitrile **2** (1 g, 2.4 mmol) was added and then refluxed for 30 min. The precipitated product was filtered and dried over phosphorous anhydride. The amide **3** ($m=8$) was obtained (0.81 g, 78%). Elemental analysis for $C_{28}H_{33}NO_3$: Calc. C 77.95, H 7.65, N 3.24; Found C 77.78, H 7.75, N 3.15%; $\nu_{\max}(\text{KBr})/\text{cm}^{-1}$ 3400, 3200, 2930, 2820, 1660, 1500, 1310, 1300. NMR measurements were not performed since this compound forms crystals which could not be dissolved in standard solvents.

Sodium 4-(4'-octyloxybiphenyl-4-yloxymethyl)benzoate 4 ($m=8$). Nitrile **2** ($m=8$) (20 g, 48.3 mmol) and sodium hydroxide (5 g, 12.5 mmol) in butanol (300 ccm) were heated at reflux for 4 days. The product was filtered, washed with anhydrous diethyl ether and dried in a desiccator over phosphorous anhydride until the butanol smell disappeared. The sodium salt **4** ($m=8$) was obtained (15.5 g, 80%). Elemental analysis for $C_{28}H_{31}O_4\text{Na}$: Calc. C 74.00, H 6.82; Found C 74.12, H 6.93%; $\nu_{\max}(\text{KBr})/\text{cm}^{-1}$ 2930, 2820, 1600, 1530, 1500, 1420, 1250. NMR measurements were not performed since this compound forms crystals which could not be dissolved in standard solvents.

4-(4'-Octyloxybiphenyl-4-yloxymethyl)benzoate esters.

Unbranched alcohols (compounds 5 and 17). To the sodium salt **4** ($m=8$) (1 g) a relevant alcohol (5 ml) in toluene (20 ml) and concentrated sulfuric acid (6 drops) were added and heated for 5 h under reflux. The reaction mixture was cooled, washed with 10% aqueous sodium carbonate and dried with magnesium sulfate. The product was chromatographed on silica gel using toluene as eluent. Yields varied from 70 to 90%.

E.g.: *n*-Butyl 4-(4'-octyloxybiphenyl-4-yloxymethyl)benzoate **5** ($n=4$). Elemental analysis for $C_{32}H_{40}O_4$: Calc. C 78.68, H 8.19; Found C 78.55, H 8.11%; $\nu_{\max}(\text{KBr})/\text{cm}^{-1}$ 2950, 2930, 1720, 1600, 1500, 1480; $\delta_{\text{H}}(\text{CDCl}_3)$ 8.41 (d, 2H), 7.57–7.38 (m, 6H), 6.98 (d, 2H), 6.92 (d, 2H), 5.12 (s, 2H), 4.32 (t, 2H), 3.96 (t, 2H), 1.81–1.65 (m, 3H), 1.56–1.22 (m, 14H), 0.97 (t, 3H), 0.89 (t, 3H); $\delta_{\text{C}}(\text{CDCl}_3)$ 166.36, 158.33, 157.49, 142.14, 134.02, 133.00, 130.02, 129.82, 127.71, 127.64, 126.90, 115.06, 114.72, 69.36, 68.04, 64.87, 31.82, 30.76, 29.38, 29.30, 29.25, 26.06, 22.67, 19.27, 14.11, 13.77.

Branched alcohols (compounds 6–16). To the sodium salt **4** (1 g, 2.2 mmol) suspended in dry toluene (20 ccm) was added oxalyl chloride (2 ml), and then the mixture was refluxed for 2 h. The precipitated sodium chloride was filtered and the filtrate evaporated to dryness. The acid chloride thus formed,

dissolved in dry toluene (10 ml), was added to a mixture of the relevant alcohol (1 ml) in pyridine (2 ml). After evaporation of the solvents the product was purified with column chromatography on silica gel using toluene as eluent. Yields varied from 50 to 70%.

E.g.: Geranyl 4-(4'-octyloxybiphenyl-4-yloxymethyl)benzoate **14**. Elemental analysis for $C_{38}H_{48}O_4$: Calc. C 80.28, H 8.45; Found C 80.15, H 8.51%; $\nu_{\max}(\text{KBr})/\text{cm}^{-1}$ 2990, 2850, 1730, 1620, 1500; $\delta_{\text{H}}(\text{CDCl}_3)$ 8.06 (d, 2H), 7.49 (d, 2H), 7.42 (dd, 4H), 6.95 (dd, 4H), 5.468 (t, 1H), 5.12 (s, 2H), 5.094 (t, 1H), 4.84 (d, 2H), 3.956 (t, 2H), 2.08–2.02 (m, 4H), 1.76 (s, 3H), 1.67 (s, 3H), 0.888 (s, 3H); $\delta_{\text{C}}(\text{CDCl}_3)$ 166.33, 158.30, 157.47, 142.35, 142.12, 134.01, 132.99, 131.80, 130.00, 129.87, 127.70, 127.64, 126.86, 123.72, 118.34, 115.05, 114.70, 69.36, 68.02, 61.89, 39.53, 31.82, 29.38, 29.30, 29.26, 26.28, 26.06, 25.68, 22.66, 16.55, 14.11.

N,N-Dioctyl-4-(4'-octyloxybiphenyl-4-yloxymethyl)-

benzamide 27. To the sodium salt **4** ($m=8$) (1 g, 2.2 mmol) in toluene (20 ml) was added oxalyl chloride (2 ml) and the reaction mixture heated for 2 h at reflux. The precipitated sodium chloride was filtered and the filtrate evaporated to dryness. The acid chloride thus formed, dissolved in toluene, was added to a solution of dioctylamine (2 g) in toluene (20 ml). After evaporation of the solvents the reaction mixture was chromatographed on silica gel using chloroform as eluent. Compound **27** was obtained (1.05 g, 73%). Elemental analysis for $C_{44}H_{65}NO_3$: Calc. C 80.61, H 9.92, N 2.13; Found C 80.49, H 10.05, N 2.16%; $\nu_{\max}(\text{KBr})/\text{cm}^{-1}$ 2940, 2830, 1670, 1500; $\delta_{\text{H}}(\text{CDCl}_3)$ 7.52–7.35 (m, 8H), 6.96 (dd, 4H), 5.11 (s, 2H), 3.98 (t, 2H), 3.47 (s, 2H), 3.19 (s, 2H), 1.79 (m, 2H).

Glycidyl 4-(4'-octyloxybiphenyl-4-yloxymethyl)benzoate **18.**

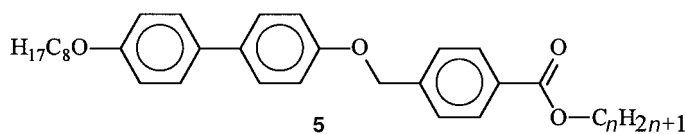
To the ester **12** (0.5 g, 0.1 mmol) dissolved in CH_2Cl_2 (5 ml) was added *m*-chloroperbenzoic acid (0.5 g, 3 mmol), and the mixture was kept overnight at room temperature. The reaction mixture was chromatographed on silica gel eluting with toluene. The epoxy ester **18** was obtained (0.21 g, 41%). Elemental analysis for $C_{31}H_{36}O_3$: Calc. C 76.22, H 7.37; Found C 76.08, H 7.48%; $\nu_{\max}(\text{KBr})/\text{cm}^{-1}$ 2950, 2830, 1720, 1530; $\delta_{\text{H}}(\text{CDCl}_3)$ 8.07 (d, 2H), 7.54 (d, 2H), 7.46 (t, 4H), 7.01 (d, 2H), 6.94 (d, 2H), 5.17 (s, 2H), 4.67 (dd, 1H, J_1 3.0, J_2 12.0 Hz), 4.18 (dd, 1H, J_1 6.0, J_2 12 Hz), 3.99 (t, 2H), 3.35 (m, 1H), 2.91 (dd, 1H, J_1 5.0, J_2 4.5 Hz), 2.74 (dd, 1H, J_1 5.0, J_2 3.0 Hz), 1.79 (m, 2H), 1.52–1.22 (m, 10H), 0.89 (t, 3H).

Preparation of halogeno derivatives of methyl 4-(4'-dodecyloxybiphenyl-4-yloxymethyl)benzoate (20 and 21). To the methyl ester **19** (1 g, 2.2 mmol) was added chlorine (or bromine) (4.4 mmol) in carbon tetrachloride at 0 °C, and the mixture was kept overnight at room temperature. Then the solvent and the excess of chlorine (or bromine) were evaporated and the product was purified *via* chromatography on silica gel using chloroform as eluent. The dichloro derivative **20** (or dibromo derivative **21**) was obtained.

For dichloro ester **20** (0.36 g, 31%). Elemental analysis for $C_{33}H_{40}O_4Cl_2$: Calc. C 69.35, H 7.00; Found C 69.45, H 7.10%; $\nu_{\max}(\text{KBr})/\text{cm}^{-1}$ 2990, 2870, 1710, 1620, 1500; $\delta_{\text{H}}(\text{CDCl}_3)$ 8.07 (d, 2H), 7.55 (d, 2H), 7.42 (m, 2H), 7.32 (m, 4H), 5.24 (s, 2H), 4.04 (t, 2H), 3.92 (s, 3H), 1.95 (t, 2H), 1.85–1.10 (m, 18H), 0.88 (t, 3H); $\delta_{\text{C}}(\text{CDCl}_3)$ 166.76, 153.75, 150.90, 141.34, 136.51, 132.32, 131.24, 129.97, 129.86, 129.82, 129.77, 128.78, 128.59, 127.27, 127.27, 127.23, 126.93, 126.67, 123.85, 114.08, 73.97, 70.21, 70.18, 52.18, 31.93.

For dibromo ester **21** (0.41 g, 36%). Elemental analysis for $C_{33}H_{40}O_4Br_2$: Calc. C 60.00, H 6.06; Found C 60.05, H 6.18%; $\nu_{\max}(\text{KBr})/\text{cm}^{-1}$ 2990, 2820, 1730, 1610, 1510; $\delta_{\text{H}}(\text{CDCl}_3)$ 8.06 (d, 2H), 7.72 (dd, 2H), 7.55 (d, 2H), 7.35 (m, 2H), 6.90 (t, 2H), 5.21 (s, 2H), 4.03 (t, 2H), 3.95 (s, 3H), 1.83 (m, 2H), 1.49–1.11 (m, 18H), 0.88 (t, 3H); $\delta_{\text{C}}(\text{CDCl}_3)$ 166.77, 154.89,

Table 1 Phase transition temperatures and thermal effects for compounds **5**



<i>n</i>	Mp/°C (thermal effect/J g ⁻¹)	Phase sequence, <i>T</i> /°C (thermal effect/J g ⁻¹)
1	144.4 (65.9)	Cry _E 169.9 (8.2) Cry _B 197.8 (8.6) S _A 208.6 (38.3) Iso
2	113.7 (37.8)	Cry _E 147.2 (7.0) Cry _B 178.2 (7.4) S _A 193.7 (36.1) Iso
3	88.7 (29.9)	Cry _K 136.7 (6.0) Hex ₁ 165.2 (7.7) S _C 167.4 (0.1) S _A 187.2 (33.5) Iso
4	80.9 (27.0)	Cry _K 134.0 (5.8) Hex ₁ 161.4 (7.0) S _C 173.1 (0.7) S _A 178.8 (31.9) Iso
5	69.6 (34.7)	Cry _K 128.6 (5.4) Hex ₁ 158.5 (6.4) S _C 171.3 (0.5) S _A 175.4 (31.1) Iso
6	65.1 (37.1)	Cry _K 127.3 (4.2) Hex ₁ 156.1 (5.6) S _C 170.7 (24.4) Iso
7	70.5 (35.8)	Cry _K 125.4 (5.3) Hex ₁ 155.0 (7.4) S _C 168.6 (32.0) Iso
8	83.1 (78.6)	Cry _K 126.3 (4.8) Hex ₁ 153.8 (6.8) S _C 165.7 (31.5) Iso

153.92, 141.54, 134.09, 123.91, 131.57, 134.40, 129.92, 129.73, 126.61, 126.52, 113.81, 113.21, 112.84, 112.64, 70.21, 69.32, 52.15, 31.91.

Preparation of mono- and di-nitro derivatives of methyl 4-(4'-dodecyloxybiphenyl-4-yloxymethyl)benzoate (23** and **22**).** To the methyl ester **19** (1 g, 2.2 mmol) was added concentrated nitric acid (10 ml) at 0 °C and the mixture was stirred for 2 h at room temperature. Then the mixture was diluted with water, extracted with butyl acetate, washed with 10% aqueous potassium hydrogen carbonate and finally the organic layer was dried with magnesium sulfate. After evaporation of the organic solvent the reaction mixture was chromatographed on silica gel eluting with CH₂Cl₂. The mono- (**23**) and di-nitro derivatives (**22**) were obtained.

For di-nitro ester **22** (0.25 g, 21%). Elemental analysis for C₃₃H₄₀N₂O₈: Calc. C 66.88, H 6.78, N 4.72; Found C 66.75, H 6.84, N 4.61%; ν_{\max} (KBr)/cm⁻¹ 2990, 2820, 1720, 1620, 1520; δ_{H} (CDCl₃) 8.10–8.02 (m, 2H), 7.98 (d, 2H), 7.67 (dd, 2H, *J*₁ 2.4, *J*₂ 8.8 Hz), 7.55 (d, 2H, *J* 8.2 Hz), 7.16 (dd, 2H, *J*₁ 8.6, *J*₂ 8.8 Hz), 5.32 (s, 2H), 4.13 (t, 2H), 3.92 (s, 3H), 1.85 (m, 2H), 1.60–1.40 (m, 18H), 0.87 (t, 3H); δ_{C} (CDCl₃) 166.59, 152.18, 151.05, 140.30, 140.20, 140.00, 131.91, 131.82, 131.60, 130.27, 130.03, 129.99, 126.53, 123.68, 123.47, 115.58, 70.56, 69.90, 52.14, 31.86.

For mononitro ester **23** (0.051 g, 4.7%). Elemental analysis

for C₃₃H₄₁NO₆: Calc. C 72.39, H 7.49, N 2.55; Found C 72.45, H 7.65, N 2.65%; ν_{\max} (KBr)/cm⁻¹ 2990, 2820, 1725, 1620, 1525; δ_{H} (CDCl₃) 8.85 (d, 2H), 7.79 (d, 1H), 7.52 (m, 4H), 7.31–7.41 (m, 2H), 7.21 (m, 2H), 5.22 (s, 2H), 4.12 (t, 2H), 3.93 (s, 3H), 1.85 (m, 2H), 1.61–1.2 (m, 18H), 0.88 (m, 3H).

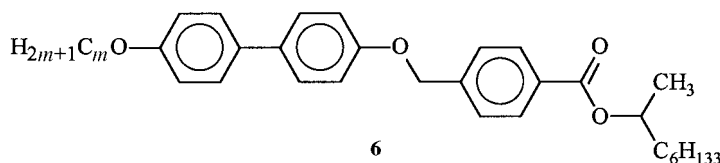
3. Results and discussion

The phase diagrams of the studied homologueous series **5–7** are shown in Fig. 1–4. The phase transition temperatures and thermal effects are collected in Tables 1 and 2 for compounds **5** and **6**, respectively, and for comparative compounds in Table 3. Preliminary data for compounds **7** were presented in ref. 8.

3.1 Non-chiral compounds **5**

Phase sequence. Molecules of homologueous series **5** have the *n*-alkyl chain attached to the carboxy moiety. The compounds of the series (Fig. 1) reveal unusually strong discrimination of the tilted phases stability upon elongation of the *n*-alkyl R¹ group. Short chain homologues (*n*=1, 2) exhibit exclusively orthogonal phases S_A, Cry_B and Cry_E. Extending the terminal chain by just one carbon atom destabilises completely the Cry_B and Cry_E phases, resulting in the sequence of tilted

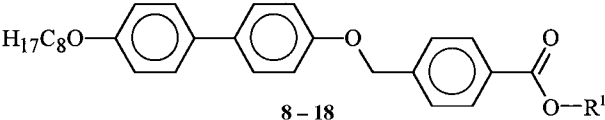
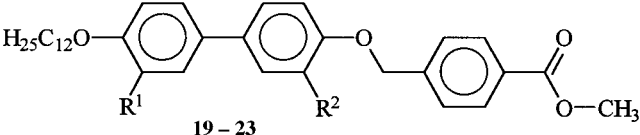
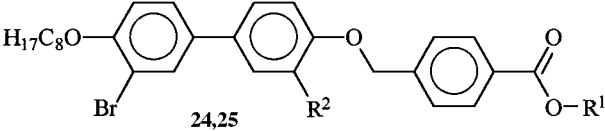
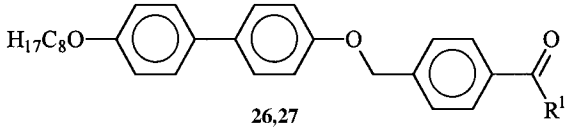
Table 2 Phase transition temperatures and thermal effects for compounds **6**



<i>m</i>	Phase sequence, <i>T</i> /°C (thermal effect/J g ⁻¹)										
	Cry		Cry _J		Hex ₁		S _{CA}		S _C		Iso
7	•	75.8 (50.9)	•	120.2 (5.4)	• ^a	127.5 (3.1)	•	134.2 (0.2)	•	138.1 (24.4)	•
8	•	53.1 (13.4)	•	104.6 (3.4)	• ^a	119.7 (3.2)	•	132.0 (0.1)	•	134.3 (24.6)	•
9	•	67.6 (23.8)	•	91.3 (3.1)	• ^a	112.5 (3.5)	•	125.3 (0.1)	•	129.1 (24.0)	•
10	•	67.9 (36.0)	•	88.3 (6.6)	• ^a	109.7 (2.8)	•	127.2	•	128.2 (24.3)	•
11	•	78.6 (52.7)	•	91.34 (8.3)	• ^a	106.6 (2.6)	•	117.8 (0.1)	•	125.4 (23.5)	•
12	•	81.2 (52.0)	•	89.5 (8.1)	• ^a	104.0 (3.4)	•	119.3 (0.1)	•	123.6 (22.6)	•
13	•	88.9 (74.3)	•	88.5 (8.0)	•	101.3 (3.5)	•		•	121.5 (22.3)	•
14	•	88.5 (79.6)	•	86.6 (8.1)	•	99.2 (2.5)	•		•	120.0 (21.8)	•
16	•	91.1 (83.0)	•	83.0 (4.8)	•	94.5 (2.4)	•		•	116.8 (19.7)	•

^aHex_{1A} phase.

Table 3 Phase transition temperatures and thermal effects for compounds **8–27**

R ¹	R ²	M _p /°C (thermal effect/J g ⁻¹)	Phase sequence, T/°C (thermal effect/J g ⁻¹)
 8–18			
8 CH(C ₈ H ₁₇) ₂	—	< room temp.	S _C 38.2 (0.16) S _A 62.1 (2.4) Iso
9 Bu ⁱ	—	< 50	Cry _J 120.8 (4.7) Hex _I 143.0 (5.2) S _C 167.8 (1.5) S _A 177.7 (27.8) Iso
10 (CH ₂) ₂ CHMe ₂	—	82 (19.1)	Cry _J 121.0 (5.0) Hex _I 147.8 (5.1) S _C 169.7 (3.1) Iso
11 CH ₂ CHMeBu	—	< room temp.	Cry _J 90.4 (7.6) Hex _I 95.0 (0.45 jump) S _C 129.2 (5.2) S _A 132.4 (15.9) Iso
12 CH ₂ CH=CH ₂	—	87.4 (32.7)	Cry _E 142.5 (6.4) Hex _I 167.3 (8.4) S _A 186.7 (34.3) Iso
13 [(<i>E</i>)-CH ₂ CMe=CHCH ₂] ₃ H	—	53.0 (14)	Hex _I 108.6 (3.8) S _C 118.4 (27.1) Iso
14 [(<i>E</i>)-CH ₂ CH=CMech ₂] ₃ H	—	64.2 (31.0)	Cry _J 112.6 (4.0) Hex _I 126.6 (2.9) S _C 136.2 (27.2) Iso
15 CH ₂ C=CH	—	111.3 (96.8)	Cry _E 137.9 (6.4) Hex _B 163.0 (7.7) S _A 176.5 (32.5) Iso
16 cyclohexyl	—	107, broad peak	Cry _J 113.5 (3.9) Hex _I 151.6 (6.9) S _C 168.3 (1.0) S _A 169.4 (28.5) Iso
17 CH ₂ CCl ₃	—	129.1 (55.4)	Cry _J 108.2 (5.2) Hex _J 121.0 (3.6) S _C (150.4 (2.0) S _A 156.3 (18.8) Iso
18 glycidyl	—	104.8 (15.5)	Cry _J 140.0 (6.5) Hex _I 152.6 (0.1) Hex _B 162.4 (9.9) S _A 177.6 (29.8) Iso
 19–23			
19 H	H	133.2 (93.9)	Cry _E 168.4 (6.9) Cry _B 193.1 (5.7) S _A 201.6 (40.0) Iso
20 Cl	Cl	80	—
21 Br	Br	65.5 (64.5)	S _A 83.9 (0.4) N 88.5 (2.4) Iso
22 NO ₂	NO ₂	122 (76.7)	S _A 142.9 (15.6) Iso
23 NO ₂	H	77 (53)	—
 24,25			
24 CH ₃	H	91.6 (31.8)	S _A 123.1 (10.0) Iso
25 Pr ⁱ	Br	70.4 (27.1)	S _A 80.7 (9.3) Iso
 26,27			
26 NH ₂	—	258 (54.8)	S _A 263 (1.6) Iso
27 N(C ₈ H ₁₇) ₂	< room temp.	S _A 62.1 (0.4) N 66.6 (3.6) Iso	

phases S_C, Hex_I and Cry_K preceded by a short temperature range where an S_A phase is observed. The inclination of the phase transition line Cry_B–Hex_I that divides orthogonal and tilted phase regions |dT/dn| is about 60 K. Details of the phase diagram topology were determined by studying binary mixtures of homologues with terminal chain length n=2 and 3 (Fig. 2). The phase sequence moving from the crystalline to hexatic smectic phases Cry_B–Hex_I observed on decreasing temperature suggests reentrant succession of liquid-like translational order. The attempts to detect the exact position of the Cry_E–Cry_K phase transition line by studies of the binary mixtures failed, since neither enthalpy changes nor clear differences in the observed textures were visible at the transition point. A phase diagram with a positive slope (dT/dn > 0) for the Cry_E–Cry_K phase transition line was proposed (Fig. 1), which does not suggest any reentrant phenomenon related to the Cry_E–Cry_K phase transition.

On DSC thermograms, phase transition S_A–Cry_B–Cry_E enthalpy peaks are sharp without noticeable pretransitional

heat capacity anomalies. The lack of any peak broadening at the S_A–Cry_B phase transition confirms its first order nature.⁹ This is in agreement with the identification of the smectic B phase as a crystal-like phase not a hexatic one. For the long chain homologues, the second order S_A–S_C phase transition reveals a characteristic heat capacity jump without a transition enthalpy peak. For the S_C–Hex_I phase transition significant heat capacity anomalies were observed, typical for the creation of long-range bond orientational order. The enthalpy changes at this transition were found to be nearly constant along the S_C–Hex_I line, similar to the enthalpy changes along the Hex_I–Cry_K borderline, since Hex_I phase stability does not depend on the terminal chain length.¹⁰

X-Ray studies. Crystallographic parameters obtained in the X-ray investigation of compounds **5** are presented in Table 4. As expected, the S_C phase without long range positional order within the smectic layer displays a diffuse signal related to the averaged intermolecular spacing. This signal becomes narrower

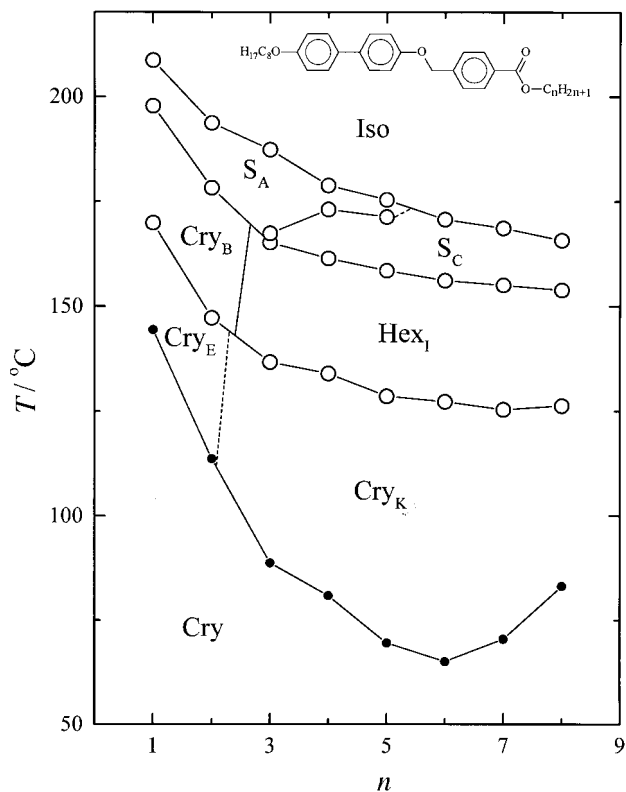


Fig. 1 Phase diagram for compounds 5.

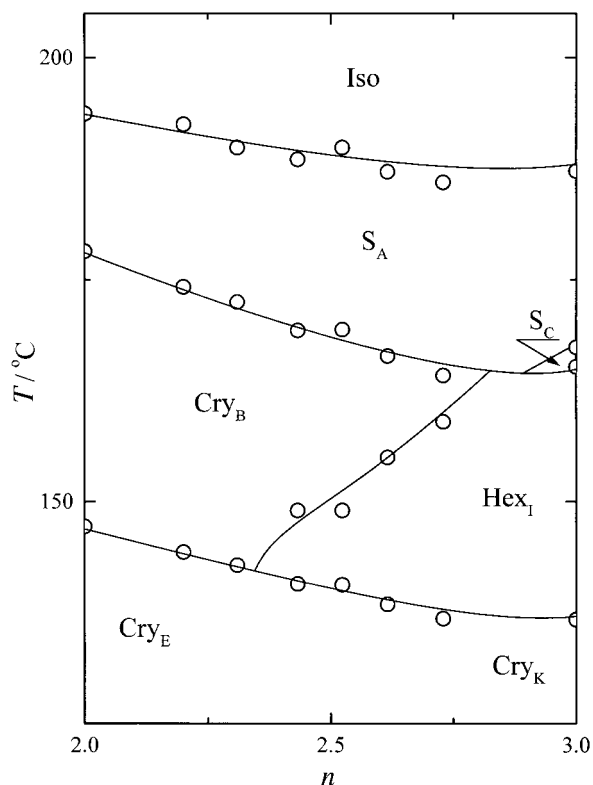


Fig. 2 Phase diagram for binary mixtures of 5 ($n=2$) and 5 ($n=3$).

and more intense in the hexatic Hex_1 smectic phase, showing an increase in the positional order to a range of hundreds of angstroms, which is for hexatic phases.¹¹ Moreover, in the Hex_1 phase the molecules become more closely packed and the X-ray reflection is slightly shifted toward a higher diffraction angle. A similar shift was also observed at the transition from the S_A to the crystalline Cry_B phase. A few rather sharp signals

found for the Cry_E and Cry_K smectic phases point to periodic long-range molecular arrangement. In the Cry_E phase, the positions of the measured peaks confirm an orthogonal rectangular crystalline lattice substantially distorted from a regular hexagon ($b:a$ ratio in Table 4). For the tilted crystalline phase Cry_K the obtained X-ray results fit rather well to the monoclinic unit cell with the tilt being towards the longer edge. Attempts to find reasonable parameters for monoclinic cells with the tilt directed to the shorter edge were not successful. Thus the sequence of tilted phases in compounds 5 is S_C - Hex_1 - Cry_K , which conserves the azimuthal direction of the tilt angle with respect to the local crystallographic axes, rather than S_C - Hex_F - Cry_H . The presence in the Cry_K and Cry_E phases of a few peaks (hkl) with non-zero l indices indicates a high degree of interlayer molecular correlation. Additionally the appearance of the (210) signal, which is detected in both the crystalline Cry_E and Cry_K phases, confirms that the molecular rotation in these phases is strongly restricted.¹² For the orthogonal Cry_B , Cry_E phases the interlayer distance is nearly equal to the molecular length ($d/L \sim 1$) with faint growth (about 0.1 Å) in the Cry_E phase.

3.2 Chiral compounds 6 and 7

Phase sequence. Compounds 6 and 7 contain in their terminal chains an asymmetric carbon atom placed next to the carboxy group. Similarly to compounds 5, substances with long ester terminal chain form exclusively tilted phases (Fig. 3 and 4): the liquid-like smectic C, hexatic smectic I and crystalline smectic J phases. Assignment of the hexatic phases as a smectic I phase followed identification based on X-ray studies performed for aligned samples of 6/7 ($m=8, n=6$).^{13†} The melting and clearing temperatures are visibly depressed with respect to those observed for compounds 5 due to steric hindrance exerted by the methyl group substituted at the chiral carbon atom. Both presented series of compounds 6 and 7 reveal tilted phases with ferroelectric or antiferroelectric⁷ properties. Strong discrimination of polar properties takes place upon changing both the chiral and achiral terminal chains. In compounds 6, in which the achiral tail is changed, homologues with $m \geq 13$ form exclusively ferroelectric phases, while in homologues with $m < 13$ antiferroelectric properties dominate (Fig. 3). In compounds 7, in which the chiral chain is modified, the odd-even effect was detected upon its elongation (Fig. 4). Compounds with odd n number of carbon atoms in chiral chain form only ferroelectric phases, while for even n antiferroelectric phases appear.

For all R enantiomers of compounds 6 and 7 in the S_C^* phase, a left-handed twist of the helix was found, as determined from left-handed circular light reflection.⁵ Taking into account the spatial configuration (R) and the parity of the asymmetric centre (odd) as well as the inductive effect of the substituted methyl group (+I), the obtained helical handedness fully complies with theoretical predictions.^{6,14}

Substances with exclusively ferroelectric phases were found to reveal a drastically different temperature dependence of the helical pitch when compared to materials forming both ferroelectric and antiferroelectric phases. For a compound with only ferroelectric phases the helical pitch was in the visible light wavelength range, and it became shorter as the temperature is reduced (Fig. 5). This decreasing of the pitch seems to be mainly connected with specific behaviour of the elastic coefficients,¹⁵ as the ratio of spontaneous polarisation to the tilt angle P_s/θ is approximately temperature independent. In compounds that exhibit a S_{CA}^* phase below the S_C^* phase, in the ferroelectric phase the helical pitch increases on approaching the S_C^* - S_{CA}^* phase transition. In the antiferroelectric phase

† Compound 6 ($m=8$)=Compound 7 ($m=8, n=6$), i.e. this compound is common to both series of homologues.

Table 4 X-Ray diffraction signals for compounds **5**, and corresponding crystallographic distances obtained from diffractograms and (in parentheses) calculated from assumed crystallographic cell

	Crystallographic distances/Å								Cell dimensions	
	(11-1)	(110)	(111)	(200)	(201)	(202)	(210)	(001)		(002)
$n=2, L=30.5$										
Cry _B		4.46 ^a						30.45	15.2 (15.2)	$a=8.93 \text{ \AA}$ $b=5.15 \text{ \AA}$ $c=30.45 \text{ \AA}$ $\alpha=\beta=\gamma=90^\circ$
Cry _E		4.56	4.45 (4.51)	4.18	4.13 (4.15)	4.07 (4.04)	3.30 (3.31)	3.50	15.3 (15.25)	$a=8.36 \text{ \AA}$ $b=5.43 \text{ \AA}$ $c=30.50 \text{ \AA}$ $\alpha=\beta=\gamma=90^\circ$ $b/a=0.649$
$n=6, L=34.9$										
S _C		4.5 ^a						32.11	16.1 (16.05)	
Hex _I		4.52 ^a						33.61	17.10 (16.85)	
Cry _K	4.67	4.54	4.35	4.21		4.02 (4.08)	3.35 (3.32)	33.61	17.09 (16.85)	$a=8.42 \text{ \AA}$ $b=5.69 \text{ \AA}$ $c=35.49 \text{ \AA}$ $\alpha=108.7^\circ$ $\beta=\gamma=90^\circ$ $b/a=0.676$

^aBroad signal.

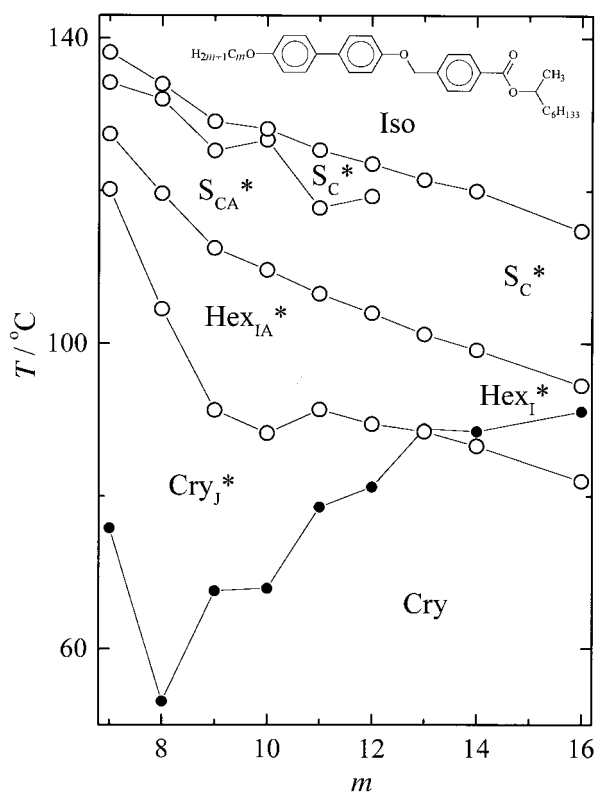


Fig. 3 Phase diagram for compounds **6**.

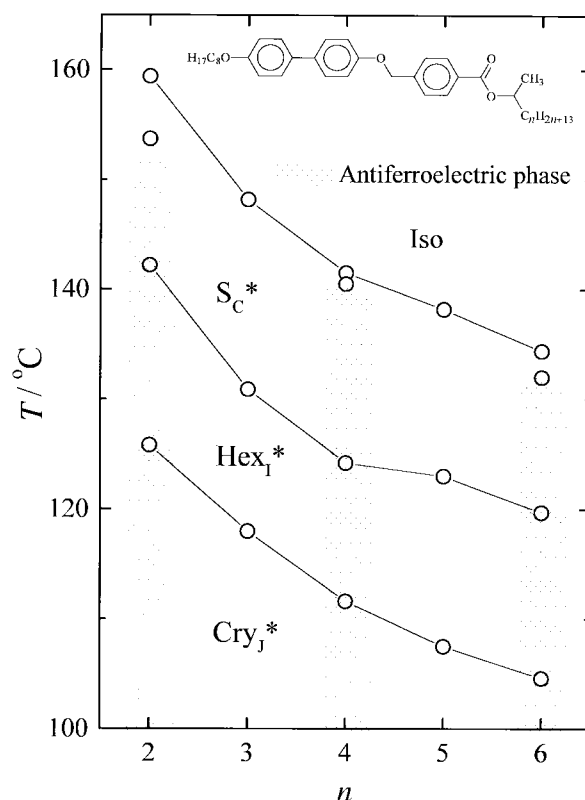


Fig. 4 Phase diagram for compounds **7**.

temperature range the helix is unwound (Fig. 5). Helix unwinding allows the appearance of the in-plane director modulations in the S_{CA}* and Hex_{IA}* phases, detected as stripe and square textures in thick (above ~10 μm) free suspended films.¹⁶

The ferro-antiferro phase transition was detected during routine DSC scans as small enthalpy (ca. 0.2 J g⁻¹ K⁻¹) peaks. In the X-ray studies no detectable changes in the smectic layer thickness at the S_C-S_{CA} phase transition were found. The plot

of layer spacing vs. temperature for compounds **6** with $m=12$ and $m=13$ is presented at Fig. 6. The phase transition into the hexatic (Hex_{IA}* or Hex_I*) phase was observed as a slight increase of the layer distance, which is probably related to the growth of the orientational order of long molecular axes in the hexatic phase.

The studied compounds have a mesogenic core structure similar to MHPOBC. However, in comparison to MHPOBC

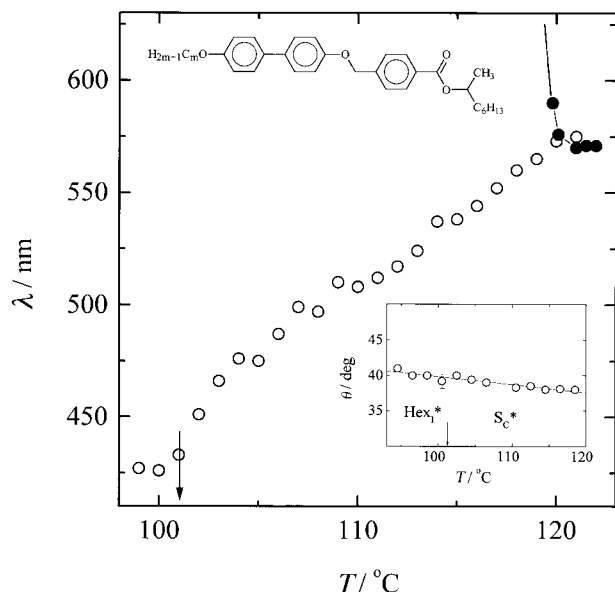


Fig. 5 Temperature dependence of selective reflection wavelength λ for compounds **6** ($m=12$) and **6** ($m=13$). Inset: tilt angle θ vs. temperature for **6** ($m=13$). Arrows indicate the Hex_1^* - S_C^* phase transition.

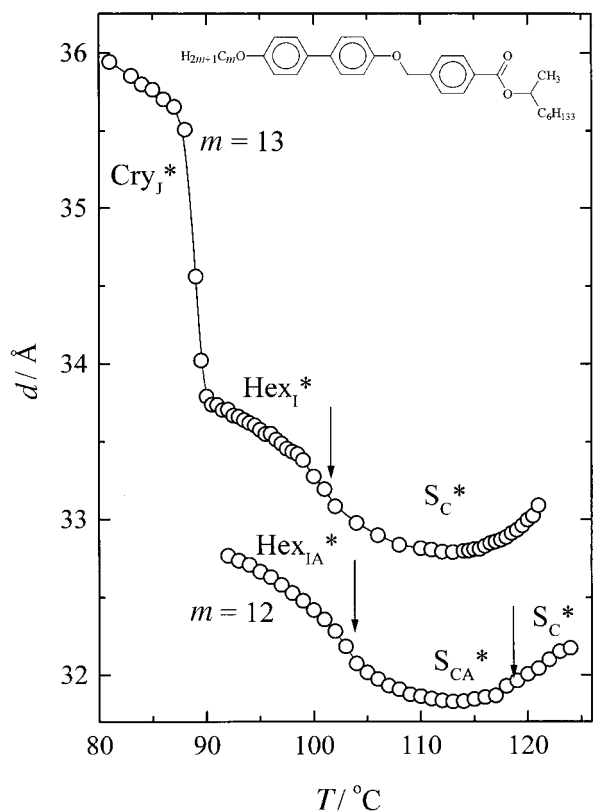


Fig. 6 Layer thickness d vs. temperature for **6** ($m=12$) and **6** ($m=13$). Arrows indicate the phase transition temperatures.

our related compound [**6/7** ($m=8$, $n=6$)] does not create a S_A phase and reveals a much broader tilted phase temperature range (ca. 80°C , for MHPOBC, ca. 57°C).⁷ Moreover, no intermediate $\text{S}_{C\alpha}^*$ and ferroelectric $\text{S}_{C\gamma}^*$ phases were observed.

Polar properties. In the studied chiral compounds a high value of the spontaneous polarisation P_s is detected in the smectic C phase, which increases slightly in the hexatic phase (Fig. 7). In the ferroelectric smectic C phase a non-threshold tilt and P_s switching is observed, while in the antiferroelectric

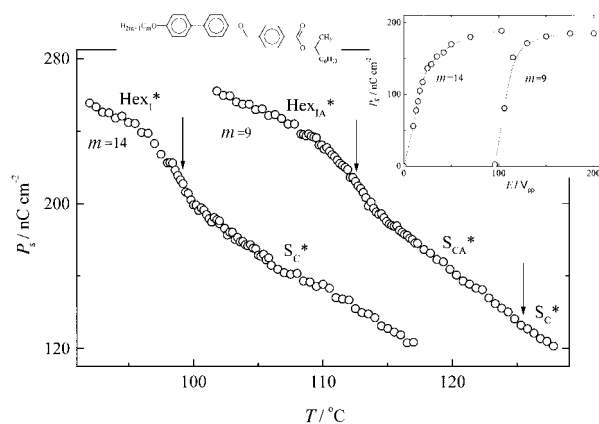


Fig. 7 Temperature dependence of spontaneous polarisation P_s for **6** ($m=14$) and **6** ($m=9$). Arrows indicate the phase transition temperatures. Inset: P_s switching curves in ferroelectric or antiferroelectric smectic C phases measured 3 K above the transition into the hexatic phase.

smectic C phase a switching onset field is observed¹⁷ (inset in Fig. 7). Using sufficiently low frequency (below 1 Hz) electric field, tristable optical switching and double current peak were resolved in the antiferroelectric phases. For the *R* enantiomers the negative sign of the spontaneous polarisation was found in both ferro- and antiferro-electric phases. This result suggests that the alkyl chain at the asymmetric atom remains predominantly in the *trans* conformation with respect to the O-C bond of the carbonyl group and implies that the molecular core tilt is stronger than the tilt of the substituted terminal chain.⁶ The high value (about 200 nC cm^{-2}) of the spontaneous polarisation shows that, apart from the dipole moment of the methyl group, the dipole moment of the carboxy group also contributes significantly to P_s . This is due to steric repulsion between the carbonyl oxygen and the methyl group that hinders rotation of the carbonyl joint. As a result, the energetically favourable conformation with the carbonyl group out the mesogenic core plane is adopted. Thus the transverse components of the dipole moments of the carbonyl oxygen group and the methyl group are summed.

The dielectric properties were also studied (Fig. 8) for compounds with antiferroelectric and ferroelectric phases. In the ferroelectric S_C^* phase a high value for the relative permittivity ($\epsilon=400$), which is usual for this phase, is observed. A two-order lower relative permittivity in the antiferroelectric phases shows that the contribution of the Goldstone mode is eliminated. A slightly higher relative permittivity in the Hex_{1A}^* than in the S_{CA}^* smectic phase probably results from a new unknown mode inherent to the hexatic phases coming into play.¹⁸ Due to tight molecular packing and the inability to trace an alternation of the measuring field, the Cry_J^* phase exhibits the smallest relative permittivity.

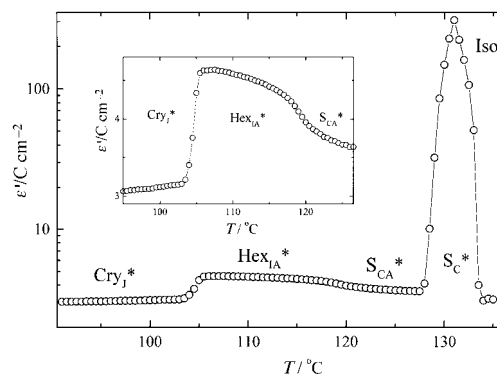


Fig. 8 Relative permittivity vs. temperature for **6** ($m=8$).

3.3 Comparative compounds

In order to discuss the influence of different substituents on mesogenicity we synthesised some compounds with modified ester terminal groups (Table 3). The replacement of the *n*-alkyl ester chain with a branched chain (compounds 8–11) lowers the tendency to form strongly crystalline smectic phases, and a sequence of S_C–Hex₁–Cry₁ smectic phases without the Cry_K phase is observed, similar to compounds 6 and 7. Moreover, as usual, the branching decreases the clearing and melting temperatures. The lowering of these temperatures is stronger for compounds 8 and 11 in which the tertiary carbon atom is closer to the mesogenic core. The branched isopropyl moiety ending the longer alkyl chains (compounds 9 and 10) influences the transition temperatures only weakly.

Insertion of a double or triple bond at the end of the short terminal alkyl chain (compounds 12 and 15) makes the molecules more rigid and promotes orthogonal smectic phases (CryE, HexB). However, the presence of a few double bonds of *E* configuration and lateral methyl groups (compounds 13 and 14) preserves the tilted phases. It should be pointed out that substitution of the methyl groups in either the odd or the even positions is not equivalent. When the methyl group is placed closer to the mesogenic core (compound 13) the mesophase stability is depressed and polymorphism is less complex.

Modification of the terminal chain by attachment of a cyclohexyl ring (compound 16) instead of an alkyl chain does not change markedly the liquid crystalline properties. In comparison to the homologue 5 (*n*=4) with comparable molecular length there is observed a similar phase sequence of orthogonal and tilted phases with slightly reduced phase transition temperatures.

The epoxy substituent (compound 18) shows an interesting hexatic phase sequence Hex_B–Hex₁, in which the tilt angle is a phase transition parameter. Microphotometry studies of the Hex_B–Hex₁ phase transition reveal discontinuous tilt changes, which indicate a first order phase transition.

Additionally, changes were made to mesogenic core structure. Bulky bromine and chlorine atoms or a nitro group were substituted onto one or two of the biphenyl rings at lateral positions. Strongly polar substituents Cl, Br, NO₂ (compounds 20–25) substantially destabilise the liquid crystalline phases. The substituted compounds reveal much lower melting and clearing temperatures than non-substituted substance 19. However, some tendency to create the S_A and N phases remains for the bromine (21, 24 and 25) and nitro (22) derivatives. Introduction of chlorine atoms (compound 20) disrupts the ordering of the molecules into mesophases completely. It is also worth noting that the dinitro-substituted material 22 exhibits mesophases while its mononitro counterpart 23 does not.

Replacement of the ester terminal chain with a primary amide group (compound 26) supports a crystal phase that is stabilised by hydrogen bonding. This results in very high melting and clearing temperatures with a rather narrow smectic A phase. Distinctly lower melting and clearing temperatures were obtained by application of a branched tertiary amide (compound 27). This compound exhibits mesogenic properties at room temperature.

4. Conclusions

The competing tendency of the functional terminal groups (–O–, –COO–) and the linkage group (–OCH₂–) to form tilted or orthogonal phases, respectively,⁶ is reflected in the observed phase sequences for compounds 5–7 and comparative compounds. For the long terminal chains with single C–C bonds the carboxy and alkoxy groups appear more influential, promoting the tilted phases. Shortening of the terminal chains gives the orthogonal phases exclusively. The use of long

terminal chains with non-conjugated double bonds does not affect the appearance of the tilted phases, whereas the introduction of the triple bond destroys the tilted phases. The branching of the terminal chains has no significant influence on the sample's ability to form the tilted phases. The replacement of the ester group by an amide (–CON=) group introduces an S_A phase. This confirms the known ability of amides substituted as the terminal outboard group to favour orthogonal phases.⁶

The destabilisation of the liquid crystal properties by the lateral moieties that were introduced into the core structure is plausibly due to the large dimensions of the substituents, which reduce the molecular shape anisotropy. The better mesostability of the disubstituted compounds over their monosubstituted counterparts seems to come from changing a potential barrier responsible for rotation about the inner phenyl–oxygen bond of the core linkage. Any moiety attached to this phenyl ring at an *ortho* position would predominantly stay in an *s-trans* conformation to the methylene fragment of the central linkage. Molecular modelling showed that the energy necessary for achieving full rotation about this bond is highest for bromine and lowest for chlorine. The potential barrier is probably high enough to restrict the rotation in bromine- and nitro-substituted molecules. It gives rise to a more rigid mesogenic core and causes better molecular alignment in the created mesophases.

We thank the Chemistry Department, Warsaw University, for financial support in the form of Grant BW-1343/21/96. Financial support from the Foundation for Polish Science Moltek 95 is also acknowledged.

References

- 1 T. Nguyen, H. Gasparoux and C. Destrade, *Mol. Cryst. Liq. Cryst.*, 1985, **123**, 271.
- 2 K. Terashima, M. Ichihashi, M. Kikuchi, K. Furukawa and T. Inukai, *Mol. Cryst. Liq. Cryst.*, 1986, **141**, 237.
- 3 J. Nakauchi, K. Sakashita, Y. Kageyama, S. Hayashi, K. Mori and S. Kenji, *Bull. Chem. Soc. Jpn.*, 1989, **62**, 1011.
- 4 G. W. Gray and J. W. G. Goodby, in *Smectic Liquid Crystals*, Leonard Hill, Glasgow and London, 1984.
- 5 P. G. de Gennes and J. Prost, *The Physics of Liquid Crystals*, Oxford Science Publications, Oxford, 1995; S. Chandrasekhar, *Liquid Crystals*, Cambridge University Press, 2nd edn., 1992.
- 6 J. W. Goodby, in *Ferroelectric Liquid Crystals*, ed. J. W. Goodby *et al.*, Gordon and Breach Science Publications, Philadelphia, 1991.
- 7 A. D. L. Chandani, E. Gorecka, Y. Ouchi, H. Takezoe and A. Fukuda, *Jpn. J. Appl. Phys.*, 1989, **L1265**, 28.
- 8 J. Mieczkowski, E. Gorecka, D. Pocięcha and M. Glogarova, *Ferroelectrics*, 1998, **212**, 357.
- 9 W. Pyzuk, A. Krowczyński, J. Szydłowska and E. Gorecka, *Liq. Cryst.*, 1995, **19**, 85.
- 10 J. Szydłowska, D. Pocięcha, A. Krowczyński and E. Gorecka, *Mol. Cryst. Liq. Cryst.*, 1997, **301**, 19.
- 11 W. Pyzuk, E. Gorecka, A. Krowczyński, D. Pocięcha, J. Szydłowska, J. Przedmojski and Li Chen, *Liq. Cryst.*, 1996, **21**, 885; E. Gorecka, Li Chen, W. Pyzuk, A. Krowczyński and S. Kumar, *Phys. Rev. E*, 1994, **50**, 2863.
- 12 A. M. Levelut, *J. Phys. Colloq.*, 1976, **37**, C3.
- 13 M. Neundorff, S. Diele, S. Ernst, S. Saito, D. Demus, T. Inukai and K. Murashiro, *Ferroelectrics*, 1993, **147**, 95.
- 14 G. W. Gray and D. G. McDonnell, *Mol. Cryst. Liq. Cryst. Lett.*, 1977, **34**, 211.
- 15 B. Zeks and R. Blinc, in *Ferroelectric Liquid Crystals*, ed. G. W. Taylor, Gordon and Breach Science publications, Philadelphia 1991.
- 16 E. Gorecka, M. Glogarova, L. Leicek and H. Sverenyak, *Phys. Rev. Lett.*, 1995, **75**, 4047; E. Gorecka, M. Glogarova, L. Leicek and H. Sverenyak, *Ferroelectrics*, 1996, **178**, 101.
- 17 A. Fukuda, Y. Takahashi, T. Isozaki, K. Ishikawa and H. Takezoe, *J. Mater. Chem.*, 1994, **4**, 997 and references cited therein.
- 18 To be published elsewhere.